Proceedings of the 2nd Croatian Conference on Earthquake Engineering - 2CroCEE
Zagreb, Croatia - March 22 to 24, 2023

DOI: https://doi.org/10.5592/CO/2CroCEE.2023.16

RELIABILITY ANALYSIS OF REINFORCED CONCRETE FRAME BY FINITE ELEMENT METHOD

Marin Grubišić[(1)], Jelena Ivošević[(2)], Ante Grubišić[(3)]

[(1)] *Assist. Professor, Faculty of Civil Engineering and Architecture Osijek, University of Osijek, marin.grubisic@gfos.hr*
[(2)] *MEng, SIRRAH Projekt Ltd, Osijek, jelenaivosevic9@gmail.com*
[(3)] *MEng, TRINAS Ltd, Osijek, ante.grubisic@trinas.hr*

Abstract

Since the prediction of the seismic response of structures is highly uncertain, the need for the probabilistic approach is clear, especially for the estimation of critical seismic response parameters. Considering the uncertainties present in the material and geometric form of reinforced concrete (RC) structures, reliability analyses using the Finite Element Method (FEM) were performed in the context of Performance-Based Earthquake Engineering (PBEE). This study presented and compared the possibilities of nonlinear modelling of the reinforced concrete (RC) planar frame and its reliability analysis using different numerical methods, Mean-Value First-Order Second-Moment (MVFOSM), First-Order Reliability Method (FORM), Second-Order Reliability Method (SORM) and Monte Carlo simulation (MCS). The calibrated numerical models used were based on the previous experimental test of a planar RC frame subjected to cyclic horizontal load. Numerical models were upgraded by random variable (RV) parameters for reliability analysis purposes, and, using implicit limit state function (LSF), pushover analyses were performed by controlling the horizontal inter-storey drift ratio (IDR). Reliability results were found to be sensitive to the reliability analysis method. The results of reliability analysis reveal that, in a nonlinear region, after exceeding the yield strength of the longitudinal reinforcement, the cross-sectional geometry parameters were of greater importance compared to the parameters of the material characteristics. The results also show that epistemic (knowledge-based) uncertainties significantly affected dispersion and the median estimate parameter response. The MCS sampling method is recommended, but the First-Order Reliability Method (FORM) applied to a response model can be used with good accuracy. Reliability analysis using the FEM proved suitable for directly implementing geometric and material nonlinearities to cover epistemic (knowledge-based) uncertainties.

Keywords: *reinforced concrete (RC) frame; cyclic response; reliability analysis; MVFOSM/FORM/SORM; Monte Carlo; OpenSees*

1. Introduction

The structural design aims to achieve structures that satisfy safety criteria, serviceability, and durability under specified service conditions. Since uncertainty is an inherent characteristic that cannot be avoided in engineering design, incorporating uncertainties in engineering design is required [1]. Reliability analysis offers a well-established theoretical framework for considering uncertainties in the engineering decision scheme. We can define reliability as the probability that a structure or system can perform a required function (or limit state function, LSF) under specified service conditions during a given period and stated conditions [2]. Conversely, the failure probability, pf (or probability of failure) is the probability that a structure does not perform satisfactorily within a given period and stated adverse conditions [3]. In the context of seismic risk analysis, the probability of exceeding the given LSF, obtained from the reliability analysis, is integrated with the seismic risk of the locality. The related term used in conjunction with seismic reliability analysis and structural risk is fragility analysis. The fragility analysis is aimed at finding the probability of a particular structural failure for different levels of intensity measures (IM) such as PGA (peak ground acceleration) or $S_A(T_1, 5\%)$ (5%-damped elastic first-period spectral acceleration), and analysis is closer to the actual estimation of structural seismic risk. Despite these fine distinctions, seismic risk, reliability, safety, and structural fragility analysis are used in various ways to denote the seismic probability of structural failure, so that the failure is defined by different structural limit state conditions [4].

Proceedings of the 2nd Croatian Conference on Earthquake Engineering - 2CroCEE
Zagreb, Croatia - March 22 to 24, 2023

DOI: https://doi.org/10.5592/CO/2CroCEE.2023.16

The most important aspect of the structural reliability analysis is the consideration of uncertainties that make a structure vulnerable to failure for a pre-defined limit state condition. The accuracy of the reliability analysis depends on how exactly all the uncertainties are considered during the analysis. First, the challenge is identifying all the sources of uncertainties; therefore, crucial uncertainties must be identified. Second, the techniques of explicit or implicit modelling are difficult to implement, therefore a certain degree of uncertainty is associated with the modelling method, with some necessary simplifications. Finally, the analytical formulation of the limit state equations and integration of the probability density function (PDF) in this domain is complex and results in various approximations. Consequently, there are different degrees of simplification in the reliability analysis leading to various reliability analysis methods, as explained below [5,6].

Considering the foregoing, the bearing capacity of the structure or element can be obtained in many ways, being the most simple and direct to use an explicit design equation, when the LSF $g(x)$ can be expressed as an explicit form or simple analytical form in terms of the basic variables x, which characterise the structural behaviour, relating the many variables, defined by probabilistic distributions. If an explicit function capable of defining the behaviour of the structure is not available, it is possible to use the FEM with implicit LSF to compute the behaviour of the structure. Such implicit LSF are encountered when the structural systems are complex and numerical analysis such as FEM must be adopted for the structural response prediction.

We can simplify the safety assessment procedure with implicit functions, by getting an explicit alternative LSF that allows a significant decrease in the response calculation time. We can obtain this function through the Response Surface Method (RSM) by fitting a surface to various realisations, for a set of variables, based on an MCS using an implicit LSF provided by the FEM [7,8]. In addition to all the well-established postulates of individual reliability methods, one of the hypotheses of this study is that even when using the FEM, the least numerical model settings can have a relatively significant impact on the reliability analysis results. These settings relate to the type of element, the plastic hinge length, the number of integration points along the element, numerical integration options for the force-based beam–column element, geometric transformation type, etc.

The described procedures in this study are compatible with the implementation of the model in the PEER PBEE framework (Pacific Earthquake Engineering Research Performance-Based Earthquake Engineering) [9,10], which besides structural responses considers the consequent functions and interaction with the Performance Assessment Calculation Tool (PACT P-58) [11]. A flexible feature of this approach is two-way communication with Python and MATLAB, which is important for applying sophisticated sampling techniques.

This paper presents the numerical calibration of the experimental RC frame model, which was later upgraded for reliability analysis. The methods of reliability analysis of MVFOSM, FORM, SORM and MCS were used, after which the basic results and conclusions were presented. All numerical analyses presented in this paper were carried out by combining OpenSees and MATLAB with customisable algorithms.

2. Experimental Model

In accordance with the prototype of a typical mid-rise building, the central bay RC frame from the ground floor was chosen and constructed at a scale of 1:2.5, which makes an aspect ratio of 1.4 [4,12,13]. Geometry, cross sections, and the amount of main longitudinal and transverse reinforcement are shown in Figure 1. The prototype of a typical building [14], from which the central frame on the scale was separated, was designed in accordance with the relevant codes [15,16], for ductility class DCM, which required concrete grade C30/37 and reinforcement B500B. The actual mechanical properties, modulus of elasticity, yielding strength, and ultimate strengths were determined in accordance with the applicable norms. After the frames were made and concrete samples were tested, the average compressive strength of the concrete cubes was 50 MPa, while the yielding and ultimate tensile strength, and the modulus of elasticity of the reinforcement were 550, 650 and 210000 MPa respectively. All these parameters of material characteristics were determined by standardised

Proceedings of the 2nd Croatian Conference on Earthquake Engineering - 2CroCEE
Zagreb, Croatia - March 22 to 24, 2023

DOI: https://doi.org/10.5592/CO/2CroCEE.2023.16

compressive and tensile tests, whose values were rounded off from a series of nine repeated tests. The model was cyclically tested in a horizontal direction, with a constant total vertical force in columns of 730 kN, i.e., 365 kN per column, to ensure an axial load ratio of 18% in each column, as defined by design (9 MPa of the axial stress relative to the gross cross-section of the column). During testing, the horizontal force was controlled, i.e., beam level displacement up to 1.0% of inter-storey drift ratio (IDR) or 14 mm, by repeating each cycle twice, resulting in damage to the ends of the columns and the beam by crushing the concrete and reaching the yield strength of individual longitudinal reinforcement.

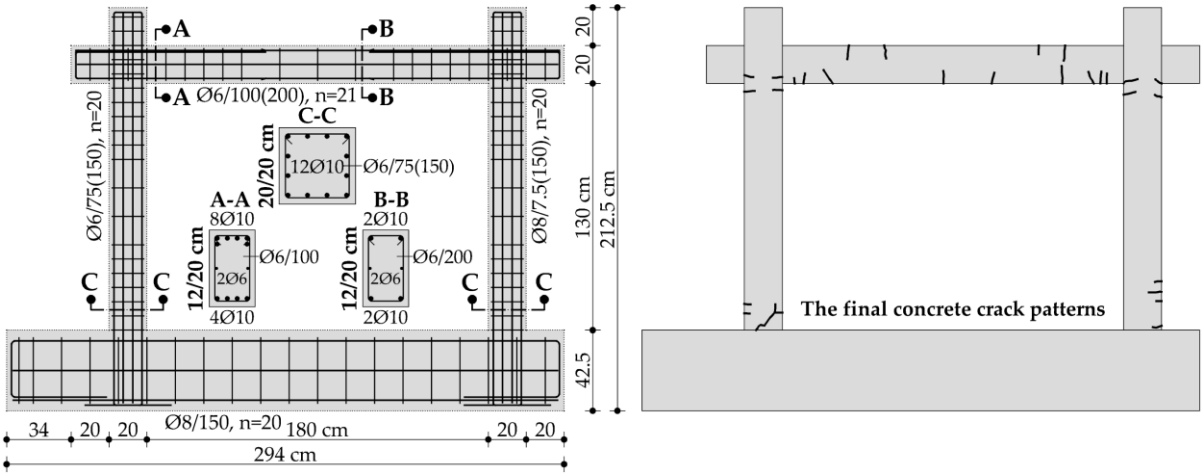

Figure 1. Schematic representation of geometry, cross sections, and the amount of reinforcement (left) and crack development during the cyclic test (right).

Figure 2 shows the hysteresis curve as a basic view of the system's behaviour, with insight into the secant stiffness (K), bearing capacity and ductility of the system and the trend of component stiffness degradation. When describing the behaviour of such models, it is necessary to evaluate the stiffness, strength, and deformation properties of individual components to numerically model the same effects and expand the analysis, such as sensitivity or reliability analysis. The specimen was not tested until the collapse but up to the targeted drift of 1.0% to preserve the specimen for further testing. The distribution and the type of cracks showed a clear flexural behaviour, with no shear failures.

The definition of the trilinear backbone curve (i.e., bearing capacity curve), which represents the three different areas of behaviour, is based on the mean value of the bearing capacity of the positive and negative horizontal direction, as shown in Figure 3.

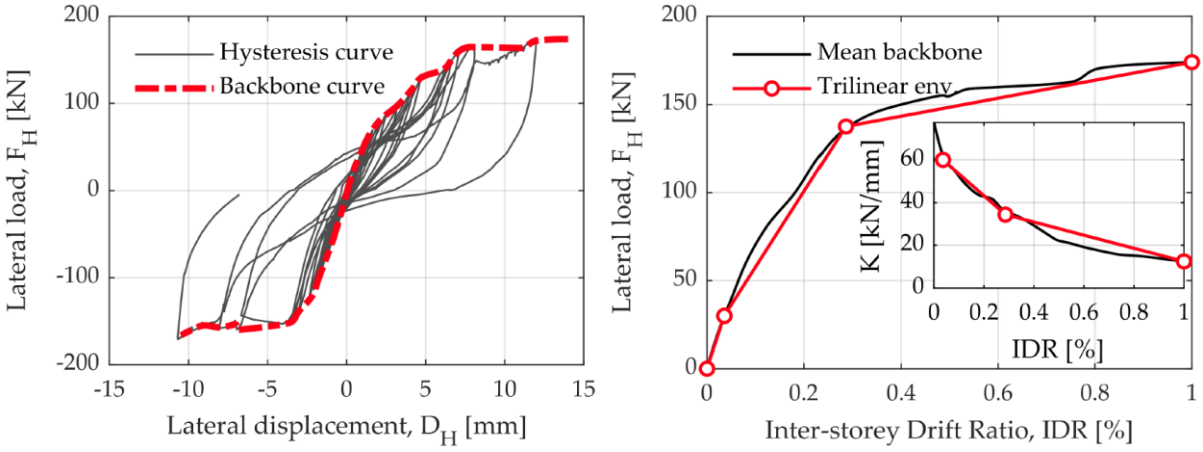

Figure 2. The hysteresis curve (left) and the average of two backbone curves as well as the secant stiffness curve, K (right).

When defining the trilinear backbone curve, the formation moment of the first significant crack was considered (1), as well as the continuation of cracks development up to the level of the global model

Proceedings of the 2nd Croatian Conference on Earthquake Engineering - 2CroCEE
Zagreb, Croatia - March 22 to 24, 2023

DOI: https://doi.org/10.5592/CO/2CroCEE.2023.16

yielding, i.e., temporary lack of bearing capacity (2) and the targeted drift (3). The characteristic points of the trilinear backbone curve and the stiffness curve were: IDR = [0.0, 0.036, 0.286, 1.0]%, FH = [0.0, 30, 137.5, 174] kN, and K = [60, 34.375, 12.428] kN/mm.

3. Numerical Model

The numerical model is constructed in two ways by the OpenSees (Figure 4) to construct as simpler a model as possible to describe the frame behaviour in relation to experimental testing. In the first part of modelling hysteresis response, a well-known approach to the theoretical semi-empirical model of concentrated plasticity (CP) was used, with hysteresis rules for RC elements according to Takeda [17], for easier and robust control of hysteresis behaviour. It should be noted that both concentrated plasticity (CP) and distributed plasticity (DP) numerical models are, by definition, suitable for reliability analysis. For this study, the DP model was chosen only because of engineering comprehension and the easier understanding of RVs and their associated coefficients of variation (COV). The nonlinearities in the CP model are defined based on the moment–rotation relationship (M–θ), which may be less understandable for practitioners, especially due to the lack of knowledge about the dispersion of these parameters at the yielding limit and ultimate bearing capacity. The nonlinearities in the DP model are defined by fibre sections, which have implemented uniaxial material behaviour parameters, based on which RVs are defined. All variables in the DP model are engineer understandable, and the dispersion of these parameters is well documented in the literature.

BeamWithHinges element was used for modelling columns and beams, which considers force-based distributed plasticity over specified plastic hinge lengths near the element ends. Two-point Gauss–Lobatto integration rule was used over the hinge regions, where the bending moments were largest, which gave the desired level of element integration accuracy [23,24]. The basic uniaxial material models were attributed to fibre cross sections to keep the model as simple as possible, but also due to certain limitations in the OpenSees program's sensitivity module at the time of the study. These uniaxial materials are Concrete01 (Kent–Scott–Park) for concrete and Steel01 (Bi-linear) for reinforcing steel. It should be emphasised that the initial modulus of elasticity of concrete directly depends on the peak strength and the associated deformation, expressed as $E_c = 2 \cdot f_{c1C}/\varepsilon_{c1C}$. Fracture energy in compression for the Kent–Scott–Park concrete model can be expressed as $G_f^c/L_p = 0.6 \cdot f_{c1C}$ $(\varepsilon_{20,C1C} - \varepsilon_{c1C} + (0.8 \cdot f_{c1C})/E_c)$. Additional introduced model parameters for the Kent–Scott–Park concrete model are elastic modulus, E_c, strain corresponding to 20% of the compressive strength, $\varepsilon_{20,C1C}$. The parameter G_f^c is the concrete fracture energy in compression (plain concrete crushing energy), which often serves for material regularisation and L_p is the plastic hinge length, which acts as the characteristic length for the purpose of providing an objective response.

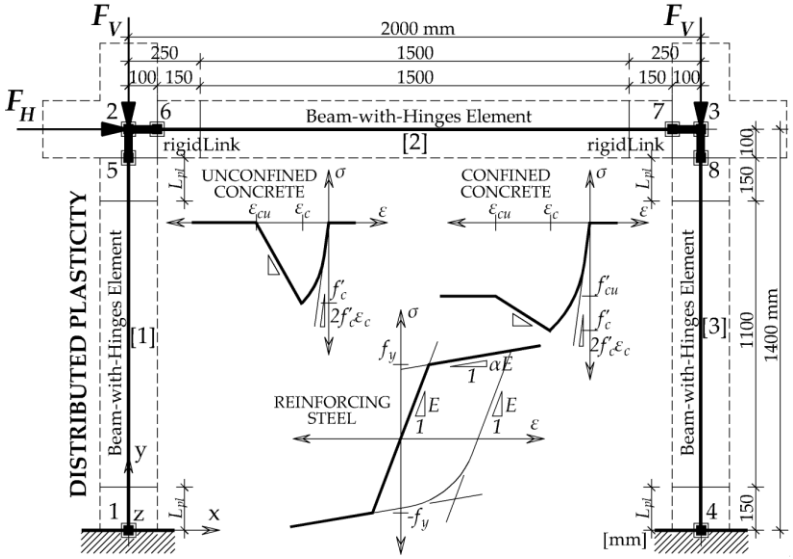

Figure 3. Distributed plasticity numerical model configuration scheme for reliability analysis

Proceedings of the 2nd Croatian Conference on Earthquake Engineering - 2CroCEE
Zagreb, Croatia - March 22 to 24, 2023

DOI: https://doi.org/10.5592/CO/2CroCEE.2023.16

The plastic hinge length was specified using an empirically validated relationship, such as the [18] equation for reinforced concrete members $L_p = 0.08 \cdot L + 0.022 \cdot f_y \cdot d_b$ [kN, mm], where L is the length of the member and f_y and d_b are yield strength and diameter, respectively, of the longitudinal reinforcing bars. The advantage of this approach is that the plastic hinge length includes the effect of strain softening and localisation as determined by experiments. Finally, the plastic hinge length was adopted as 150 mm for columns and beam. Since the parameters E_c and G_f^c are directly related to f_{c1C} and ε_{c1C}, they are not further considered RVs, as defined below. The confinement factor for columns and beams was adopted as a rounded value of 1.15, for a given cross-sectional configuration and transverse reinforcement spacing (which is closed at 135 degrees). The corotational geometric transformation was also applied in the DP model to consider the second-order effects [19–22]. The beam–column joints were considered rigid, as well as the base of the columns with a foundation. Detailed information on the parameters and settings for reliability analysis are given below.

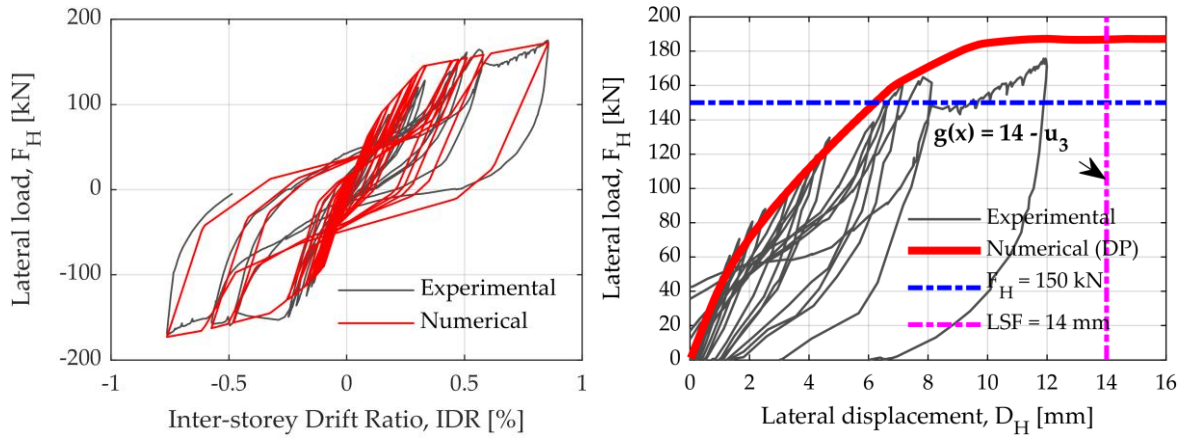

Figure 4. Comparison of hysteresis curve with pushover curve for distributed plasticity model (DP), with corresponding drift limit and horizontal load level at reinforcement yielding.

4. Reliability Analysis Results

The calibrated numerical model shown was upgraded with defined RVs of normal (N) and log-normal (LN) distributions and defined parameters associated with RVs. It should be emphasised that the numerical model was adapted to the extent that its elements or sections were defined as fibre sections, therefore not defined by springs, whose characteristics were also derived from the fibre cross-sectional analysis. This was an easier understanding of RVs and their associated parameters. As RVs, we wanted to define the parameters of material characteristics, cross-sectional geometry, depth of the concrete cover, etc. compared to the parameters of the concentrated plasticity or the pair of the moment–rotations (which is not a limit, but an intuitive approach has been adopted). The definition of RVs primarily refers to parameters of material properties of concrete and reinforcing steel and then the geometrical characteristics of the cross-section and the width and height of the RC frame. The mean values of all RVs were obtained from the experiments and calibrations, while their coefficients of variation (COV) were obtained partly from experimental material testing by comparing available literature (Table 1).

To present the possibilities of reliability analysis by FEM, a correlation between individual parameters or RVs was introduced. For example, a correlation was introduced between the yielding strength and the modulus of elasticity of reinforcing steel as 60% correlation, as obtained from the literature [25,29,30]. A complete correlation was found between the peak compressive strength of concrete for the concrete cover and core (i.e., unconfined and confined concrete section) and for the associated deformation, as 100% [25]. Thus, the importance of some RVs for the LSF could be ranked according to two parameters: $\boldsymbol{\alpha}$ and $\boldsymbol{\gamma}$ (Importance vectors). Thus, the importance vector $\boldsymbol{\alpha}$ does not consider the correlation between RVs, while the importance vector $\boldsymbol{\gamma}$ considers the defined correlation. In Table 1, the symbols of the parameters show the reinforcing steel yield strength (f_y), the elasticity modulus of the reinforcing steel (E_s), the compressive strength of the confined concrete core with corresponding

Proceedings of the 2nd Croatian Conference on Earthquake Engineering - 2CroCEE
Zagreb, Croatia - March 22 to 24, 2023

DOI: https://doi.org/10.5592/CO/2CroCEE.2023.16

deformation (f_{c1C}, ε_{c1C}), the compressive strength of the unconfined concrete with corresponding deformation (f_{c1U}, ε_{c1U}), the confined concrete crushing strength with corresponding deformation (f_{c2C}, ε_{c2C}), the unconfined concrete crushing strength with corresponding deformation (f_{c2U}, ε_{c2U}), the vertical load per column (F_v), the length of the columns and beam (L_{column}, L_{beam}), the depth of the concrete cover for both columns and beams (c_{cover}), the cross section depth of the columns and beam (H_{column}, H_{beam}) and plastic hinge length for both columns and beam (L_p).

Table 1. Summary of RVs with their mean values (μ_i), standard deviations (σ_i) and coefficients of variation (COV).

RV_i	Param.	Mean, μ_i	St. Dev., σ_i	COV	Units	Distr.	References for COV
101	f_y	550	44	0.08	[MPa]	LN	Exp. + [9–11]
102	E_s	210 000	12 600	0.06	[MPa]	LN	Exp. + [8,9,12]
103	f_{c1C}	–57.5	–8.63	0.15	[MPa]	N	Exp. + [9,13–16]
104	ε_{c1C}	–0.005	–0.0008	0.15	[–]	N	Exp. + [9,13–17]
105	f_{c1U}	–50	–7.5	0.15	[MPa]	N	Exp. + [9,12,15,16]
106	ε_{c1U}	–0.002	–0.0003	0.15	[–]	N	Exp. + [9,13,17]
107	f_{c2C}	–11.5	–2.3	0.20	[MPa]	N	Exp. + [9,13–16]
108	ε_{c2C}	–0.0085	–0.0017	0.20	[–]	N	Exp. + [9,13–17]
109	f_{c2U}	–10	–2	0.20	[MPa]	N	Exp. + [9,13,15,16]
110	ε_{c2U}	–0.0035	–0.0007	0.20	[–]	N	Exp. + [9,13,17]
111	F_v	365	36.5	0.10	[kN]	N	Exp. + [11,14]
112	L_{column}	1400	–	0.01	[mm]	N	[9,14,18]
113	c_{cover}	15	–	0.25	[mm]	N	[9,14,18]
114	H_{column}	200	–	0.05	[mm]	N	[9,14,18]
115	H_{beam}	200	–	0.05	[mm]	N	[9,14,18]
116	L_{beam}	2000	–	0.01	[mm]	N	[9,14,18]
117	L_p	15	–	0.10	[mm]	N	[9,14,18]

Material and geometric nonlinear parameters, formulation of boundary conditions, static indeterminacy, and several DOF are already defined within the numerical model, so the evaluation of RVs and the implicit LSF for the calculation of structural responses is more straightforward regarding defining explicit LSF. Figure 4 (right) shows the pushover curve of a fibre-based numeric model regarding the cyclic response of the experiment. In the exact figure, the IDR limit is defined for the ultimate LSF. In addition, the constant horizontal load value of 150 kN was adopted, which for this deterministic model is the amount of horizontal load at which the yielding strength is exceeded of reinforcing steel, after which the RC frame progressively loses its horizontal load bearing capacity. Thus, the limit state of the displacement is limited to 14 mm or 1.0% IDR.

The aim of all reliability analyses is to verify their comparability and applicability; thus, for Monte Carlo simulation (MCS), we expect the probability of $\boldsymbol{p_f}$ for a reasonable number of simulations ($N_{MCS} \geq 10^5$) close to FORM and SORM analyses. The SORM method improves the assessment given by FORM by including information about the curvature, approximating the nonlinear LSF (related to the second-order derivatives of the LSF with respect to the basic variables), while FORM approach approximates the LSF with a linear function.

4.1. MVFOSM, FORM, and SORM Analyses

Table 2 shows the difference in the order of importance vectors with and without a defined correlation. The values of $\boldsymbol{X_i^*}$ show the values of individual parameters for the same horizontal load of 150 kN reaching exactly the Design Point response, defined by the LSF and in this case was 14 mm or 1.0% of IDR. The pushover curves with the mean values of all parameters, and the design point values, are shown below for all MCS. The values of $\boldsymbol{X_i^*}$ can also optimise the system in such a way that the iterative procedure monitors the mean value difference $\boldsymbol{\mu_i}$ regarding design point values $\boldsymbol{X_i^*}$, thereby rationalising

Proceedings of the 2nd Croatian Conference on Earthquake Engineering - 2CroCEE
Zagreb, Croatia - March 22 to 24, 2023

DOI: https://doi.org/10.5592/CO/2CroCEE.2023.16

specific cross-section dimensions, frame geometry or mechanical properties of the material (reliability-based design optimisation). It is important to emphasise that the list of parameters of RV, ranked by the importance vectors, is certainly sensitive to specific implicit LSF, i.e., the order of importance vectors does not apply to any other pre-defined LSF, which is visible from the Tornado Diagram Analysis (TDA). In addition, most design solutions will remain in the linear range of behaviour throughout their lifetime, where the optimisation of such linear systems would be even more straightforward, and there would be no significant between individual LSFs regarding the importance of some RVs if the structure behaves linearly. Correlation affects not only the parameters it relates but also all the parameters with which they interact within a numerical model.

Table 2. The rank of RVs and parameters by importance vectors, obtained from the FORM analysis, according to the $\boldsymbol{\gamma_i}$ vector, i.e., *considering* the correlation between the defined RVs for the LSF $g(x) = 14.0 - u_3$.

RV_i	Param.	Units	Mean, μ_i	Design Point, X_i^*	Importance, γ_i	Importance, α_i
103	f_{c1C}	[MPa]	$-5.750 \cdot 10^{1}$	$-3.789 \cdot 10^{1}$	0.460179	–0.714091
114	H_{column}	[mm]	$2.500 \cdot 10^{2}$	$2.322 \cdot 10^{2}$	–0.449068	–0.374476
104	f_{c1U}	[MPa]	$-5.000 \cdot 10^{1}$	$-3.296 \cdot 10^{1}$	0.400155	–0.047072
116	L_{beam}	[mm]	$2.000 \cdot 10^{3}$	$2.023 \cdot 10^{3}$	0.346749	0.289152
101	f_y	[MPa]	$5.500 \cdot 10^{2}$	$5.092 \cdot 10^{2}$	–0.336795	–0.324799
113	c_{cover}	[mm]	$1.500 \cdot 10^{1}$	$1.733 \cdot 10^{1}$	0.245127	0.204410
115	H_{beam}	[mm]	$2.000 \cdot 10^{2}$	$1.922 \cdot 10^{2}$	–0.220742	–0.184076
109	ε_{c2C}	[–]	$-8.500 \cdot 10^{-3}$	$-8.500 \cdot 10^{-3}$	0.214387	–0.251653
111	F_v	[mm]	$-3.650 \cdot 10^{5}$	$-3.420 \cdot 10^{5}$	0.116115	–0.096828
112	L_{column}	[mm]	$1.400 \cdot 10^{3}$	$1.405 \cdot 10^{3}$	0.092027	0.076741
110	ε_{c2U}	[–]	$-3.500 \cdot 10^{-3}$	$-3.500 \cdot 10^{-3}$	0.088277	–0.010384
102	E_s	[MPa]	$2.100 \cdot 10^{5}$	$1.992 \cdot 10^{5}$	–0.087742	–0.058500
107	f_{c2C}	[MPa]	$-1.150 \cdot 10^{1}$	$-1.150 \cdot 10^{1}$	0.015339	–0.023803
108	f_{c2U}	[MPa]	$-1.000 \cdot 10^{1}$	$-1.000 \cdot 10^{1}$	0.013338	–0.001569
105	ε_{c1C}	[–]	$-3.500 \cdot 10^{-3}$	$-4.001 \cdot 10^{-3}$	0.008499	–0.011096
117	L_p	[mm]	$1.500 \cdot 10^{2}$	$1.507 \cdot 10^{2}$	0.007419	0.006187
106	ε_{c1U}	[–]	$-2.000 \cdot 10^{-3}$	$-2.286 \cdot 10^{-3}$	0.004856	–0.000571

At the cross-sectional level, maximum compressive strength of the confined and unconfined concrete, f_{c1C} and f_{c1U}, the total height of the beam and columns cross-section, H_{column} and H_{beam}, the depth of the concrete cover for both columns and beams affecting the effective height of the cross sections, c_{cover} and yield strength of reinforcing steel, f_y were the most sensitive parameters for the main LSF, considering the correlation between the parameters. Since the characteristics of reinforcing steel affect the behaviour of the confined concrete, the parameter f_{c1C} became the most important parameter for the LSF $g(x) = 1.0\% \cdot L_{column} - u_3$.

SORM analysis was also performed in two ways: by adopting the First Principal Curvature, SORM-FP, and by applying Curvature Fitting by combining 10 curvatures for a better approximation of the SORM-CF reliability index. The difference in the reliability index of β_{FORM} and $\beta_{SORM-CF}$ was only 0.13%, thus, the probability of the limit state exceeds $p_{f,\mathrm{FORM}} = 0.079\%$ or $p_{f,\mathrm{SORM\text{-}CF}} = 0.078\%$.

In Table 3, the reliability indexes for MVFOSM, FORM, SORM-FP and SORM-CF were compared for the 14 mm, 10 mm, and 6 mm horizontal displacements as LSF. During these analyses, it was concluded that the ranks of important parameters based on $\boldsymbol{\alpha_i}$ and $\boldsymbol{\gamma_i}$ vectors were not the same for all three LSF, which is common for nonlinear systems since not all parameters equally affect the predominantly linear and nonlinear part of the model response. Based on these conclusions, a tornado diagram is constructed [32,41–43], by applying displacement control as deterministic sensitivity.

It is worth mentioning that the values of the reliability index, β in Table 4 for FORM and SORM analysis, are less than the guidelines for Eurocode 0 for residential and office buildings.

Proceedings of the 2nd Croatian Conference on Earthquake Engineering - 2CroCEE
Zagreb, Croatia - March 22 to 24, 2023

DOI: https://doi.org/10.5592/CO/2CroCEE.2023.16

Table 3. Comparison of the reliability indexes (and their probabilities) for MVFOSM, FORM, SORM-FP and SORM-CF analysis for three different LSFs.

Analiza	**Indeks pouzdanosti, β**	**LSF #1, D_H = 14 mm**	**LSF #2, D_H = 10 mm**	**LSF #3, D_H = 6 mm**
MVFOSM	β_{MVFOSM} ($p_{f,MVFOSM}$)	4.816 ($7.338 \cdot 10^{-4}$)	2.511 ($6.028 \cdot 10^{-3}$)	0.205 ($4.186 \cdot 10^{-1}$)
FORM	β_{FORM} ($p_{f,FORM}$)	3.161 ($7.868 \cdot 10^{-4}$)	2.304 ($1.062 \cdot 10^{-2}$)	0.318 ($3.751 \cdot 10^{-1}$)
SORM–FP	$\beta_{SORM-FP}$ ($p_{f,SORM-FP}$)	3.161 ($7.868 \cdot 10^{-4}$)	2.304 ($1.062 \cdot 10^{-2}$)	0.318 ($3.751 \cdot 10^{-1}$)
SORM–CF	$\beta_{SORM-CF}$ ($p_{f,SORM-CF}$)	3.165 ($7.752 \cdot 10^{-4}$)	2.310 ($1.045 \cdot 10^{-2}$)	0.321 ($3.741 \cdot 10^{-1}$)

According to Eurocode 0 [44], the recommended minimum value for the reliability index, β (ultimate limit states) for Consequences Class 2 (CC2), that is Reliability Class 2 (RC2) and 50 years reference period is $\beta_{EC0,RC2} = 3.8$ or $p_f \approx 7.2 \cdot 10^{-5}$.

4.2. Monte Carlo Simulations

The results of the Monte Carlo analysis (conventional brute-force Monte Carlo) for the 10,000 simulations are presented below, carrying out a nonlinear analysis with Load Control (LC) of 150 kN in 40 steps per 5 kN (Figure 7). Figure 7 shows values of log-normal (LN) mean (β_{LN}) and standard deviations (θ_{LN}), and the diagrams are normalised based on horizontal force. The difference between the red and blue pushover curves should be noted. The red pushover curve was derived using the arithmetic mean values of all RV parameters.

Table 4. Comparison of the number of Monte Carlo Simulation (MCS-LC), together with the FORM analysis, on the exceedance probability of an LSF.

Total MCS, N_{MCS}	**LSF #1, D_H = 14 mm, $p_{f,MCS}$**	**LSF #2, D_H = 10 mm, $p_{f,MCS}$**	**LSF #3, D_H = 6 mm, $p_{f,MCS}$**	**Running Time MCS (h:m:s)**
1 000 (10^3)	0.0008	0.0048	0.3288	0:00:04
10 000 (10^4)	0.0006	0.0064	0.3077	0:00:39
100 000 (10^5)	0.0008	0.0068	0.3058	0:06:23
500 000	0.0008	0.0072	0.3024	0:35:20
$p_{f,MVFOSM}$	0.0000	0.0060	0.4186	0:00:01
$p_{f,FORM}$	0.0008	0.0106	0.3751	0:00:03
$p_{f,SORM-FP}$	0.0008	0.0106	0.3751	0:00:06
$p_{f,SORM-CF}$	0.0008	0.0105	0.3741	0:00:19

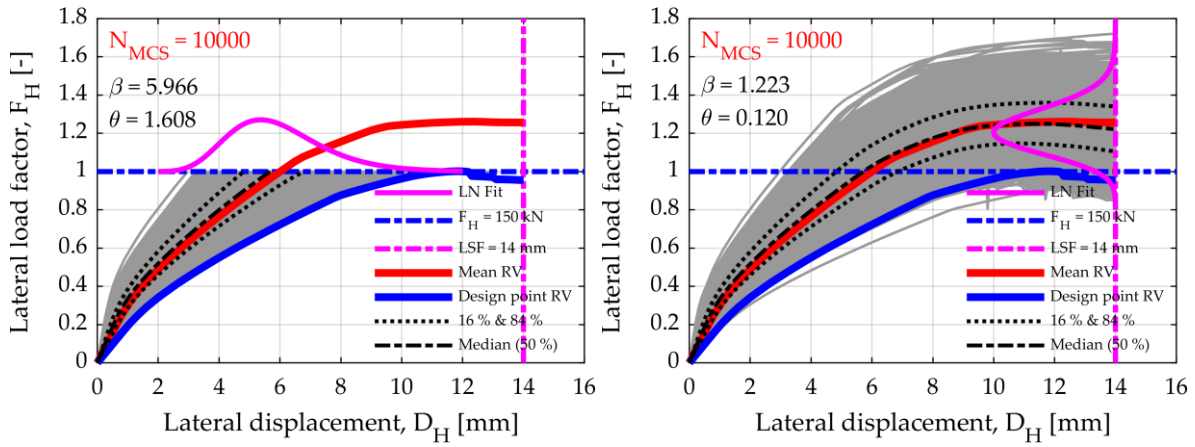

Figure 5. Illustration of MCS, for $N_{MCS} = 10^4$ simulations, load control MCS-LC (**left**) and displacement control MCS-DC (**right**)

Proceedings of the 2nd Croatian Conference on Earthquake Engineering - 2CroCEE
Zagreb, Croatia - March 22 to 24, 2023

DOI: https://doi.org/10.5592/CO/2CroCEE.2023.16

The blue pushover curve was based on the RV parameters obtained by FORM analysis ($\boldsymbol{X_i^*}$ values based on the Design Point) regarding the default LSF $g(x) = 1.0\% \cdot L_{column} - u_3$. As a by-product, FORM analysis provided importance measures ($\boldsymbol{\alpha}_i$ and $\boldsymbol{\gamma}_i$ vectors in Tables 2 and 3) to rank the uncertain parameters according to their relative influence on the structural reliability index, β. Based on these importance vectors, FORM optimised the values of all RVs ($\boldsymbol{X_i^*}$values), in which combination exactly reached the Design Point (DP) or Most Probable Point (MPP). Thus, the difference between red and blue pushover curves is necessary and presents a useful product of the FORM analysis.

The tornado diagrams (Figure 6) were also constructed by applying the displacement control (DC) pushover analysis for deterministic sensitivity, which has become commonplace in reliability analysis of the field of earthquake engineering [31,32,41–43,47,48]. The TDA is a first-order sensitivity analysis. It comprises a set of horizontal bars, one for each input RV, whose lengths represent the variation of the EDP due to each considered input RV. The diagram is intuitive to read, and it helps the analyst identify which parameters to focus on. Each input variable is set to its median value (50th percentile), and the output is measured, establishing in this way a baseline output. One by one, each input parameter is fixed to both high and low extreme values of their probability distributions (generally corresponding to the 16th and 84th percentile, especially if the input distributions are different). The input parameters are ranked according to their absolute response difference (also called "swing") so that the larger swing belongs to the variable producing the most significant uncertainty [43]. Repeated analyses observe the difference in the model response; in this case, the horizontal bearing capacity was represented in the percentage of response difference regarding the median pushover curve.

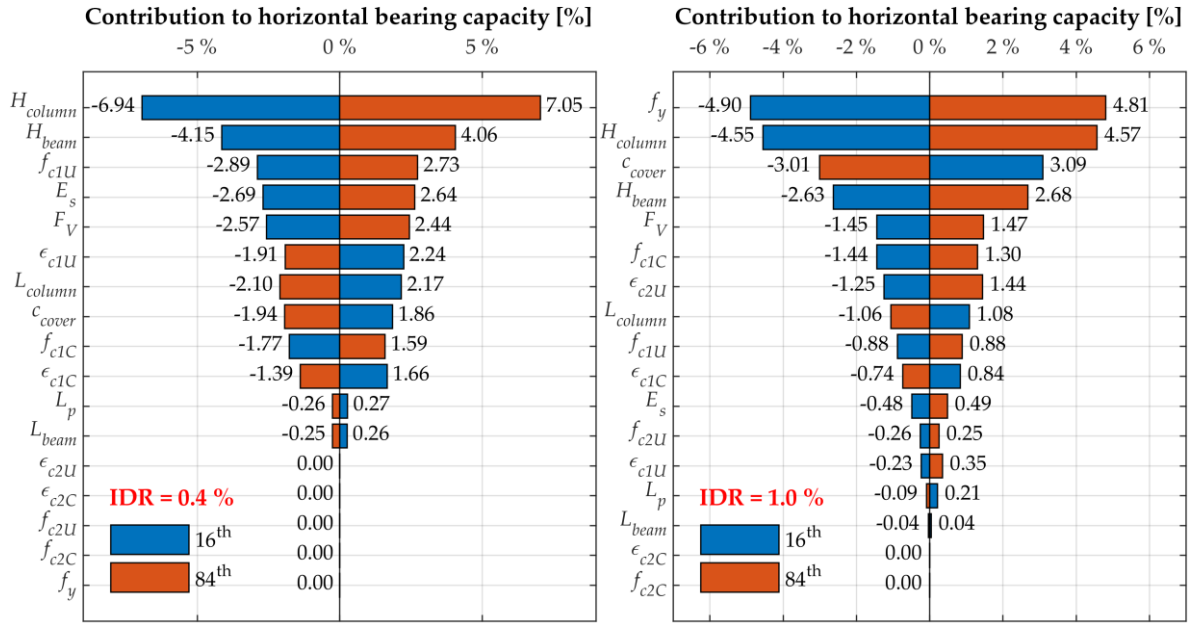

Figure 6. Tornado diagrams for three LSFs, showing the contribution of individual variables to horizontal bearing capacity, for IDR = 0.4% (**left**) and IDR = 1.0% (**right**)

Figure 7 shows the sensitivity of individual RV in the form of a standard deviation relative to the horizontal displacement, D_H. It is interesting to see when specific parameters were activated with their contribution to the system's bearing capacity. Notice the parameter f_y at a horizontal displacement of 6 mm (0.43% IDR). Almost the same trend had the crushing concrete parameters f_{c2C}, f_{c2U}, ε_{c2C}, ε_{c2U}. It is interesting that almost none of the parameters related to the properties of concrete had a linear median curve due to significant softening effects. The following limits are also shown in Figure 7: the maximum reached compressive strength limit of the unconfined concrete, f_{c1U} and ε_{c1U}, the reinforcement yield strength limit, f_y, and the limit as the beginning of concrete crushing, f_{c2C}, f_{c2U}, ε_{c2C} and ε_{c2U}.

Proceedings of the 2nd Croatian Conference on Earthquake Engineering - 2CroCEE
Zagreb, Croatia - March 22 to 24, 2023

DOI: https://doi.org/10.5592/CO/2CroCEE.2023.16

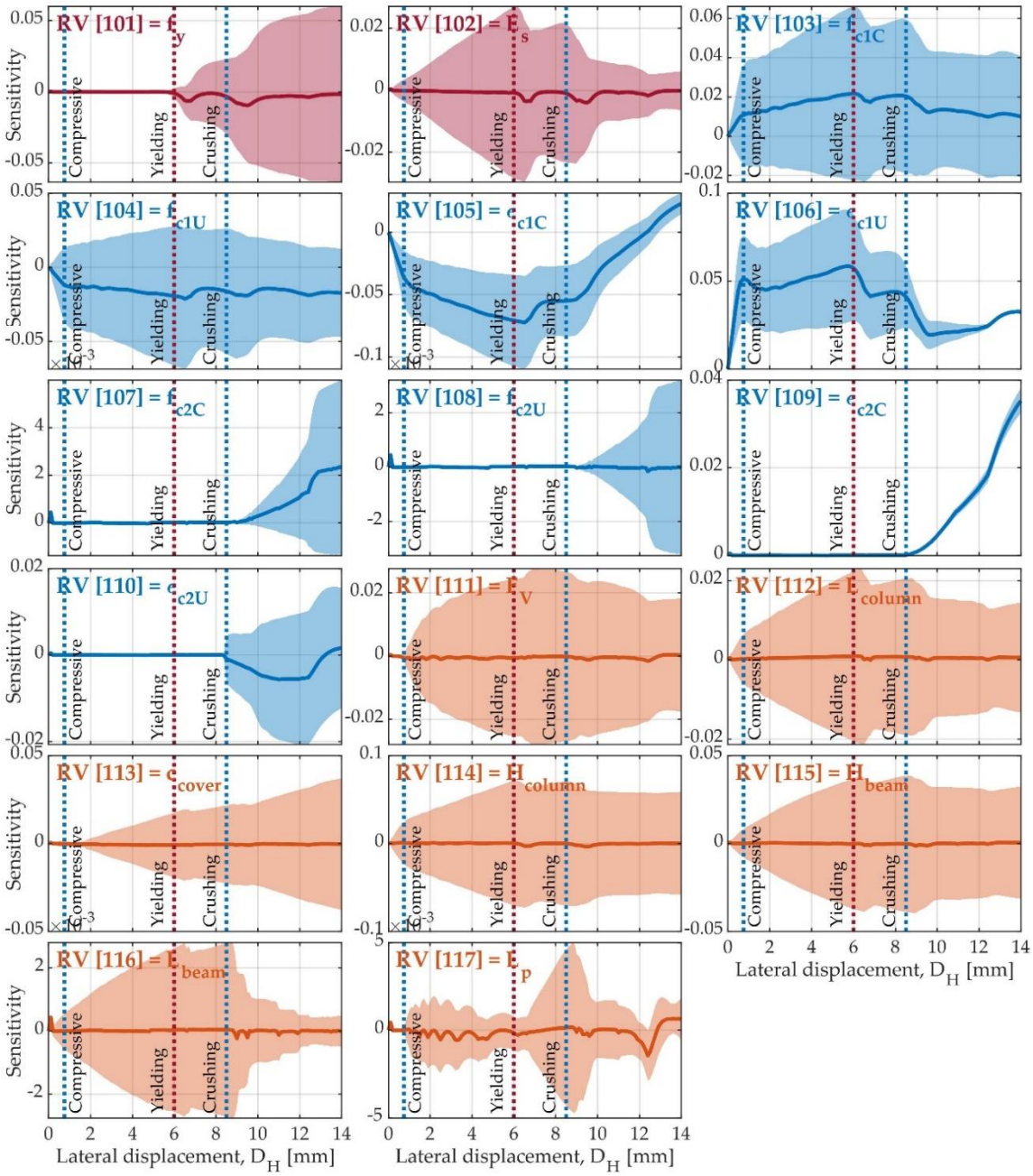

Figure 7. Overview of the sensitivity of individual RV on the nonlinear response of the RC frame (MCS-DC)

In the predominant linear range of system behaviour (0.4% IDR), the effect of significant parameters responsible for influencing the initial stiffness of the system, such as H_{column}, H_{beam}, f_{c1U}, ε_{c1U}, E_s, F_V, L_{column} and c_{cover} is visible. Parameters of crushed confined concrete did not contribute to any of the LSFs shown. For 0.4% IDR, the parameter f_y did not affect the system's bearing capacity, as expected, while for 1% IDR it was the main significant parameter affecting the system's capacity. In the linear range, it is evident that the geometrical characteristics of the cross sections were the main contributors to the system's bearing capacity (H_{column} and H_{beam}) and the stiffness of constituent materials expressed as elastic modulus (E_s and E_c defined as $E_c = 2 \cdot f_{c1C/U}/\varepsilon_{c1C/U}$).

Proceedings of the 2nd Croatian Conference on Earthquake Engineering - 2CroCEE
Zagreb, Croatia - March 22 to 24, 2023

DOI: https://doi.org/10.5592/CO/2CroCEE.2023.16

5. Conclusions

This paper describes the reliability analyses of the RC frame by the FEM. The numerical model was based on and calibrated based on experimental testing of the single-bay single-storey planar RC frame at a scale of 1:2.5. The numerical model is shown in two variants, the nonlinear elements of which are defined by rotational springs (concentrated plasticity), and by the uniaxial fibre cross sections (distributed plasticity). The calibration of the numerical model was based on the cyclic hysteretic response of the frame, while the reliability analyses were based only on the pushover bearing curve obtained by pushing the frame monotonously and unilaterally.

The ability to apply reliability analysis on a completely nonlinear numerical model using FEM and the comparability of MVFOSM, FORM, SORM-FP and SORM-CF methods with MCS is what makes this study innovative. The MVFOSM analysis overestimated the reliability index β_{MVFOSM} by up to 52% compared to the FORM and SORM analyses that have proven comparable to the MCS. The FORM analysis gives insight into the importance of some parameters through the importance vectors without considering correlation ($\boldsymbol{\alpha_i}$) and considering correlation ($\boldsymbol{\gamma_i}$). The SORM analysis with respect to the FORM analysis gave a smaller difference in the reliability index of the individual LSF, and that order was 0.13%, which is negligible. MCS gave accurate exceedance probabilities (p_f) of LSF for the number of simulations greater than $N_{MCS} \geq 10^5$, whereas this required number of simulations is expected to be significantly reduced by using sophisticated sampling techniques such as LHS. Significant parameters for the main LSF that is $g(x) = 1.0\% - u_3$ (horizontal statistics), based on the importance vectors $\boldsymbol{\gamma_i}$, are: f_{c1C} peak compression strength of the confined concrete (core), H_{column} total depth of the column cross-section, f_{c1U} peak compression strength of the unconfined concrete (cover), L_{beam} beam length, f_y tensile yield strength of reinforcing steel, and c_{cover} depth of the concrete cover directly affecting the effective cross-sectional depth.

As shown in Table 2, it is interesting that the beam length, L_{beam}, and thus the frame span, was the fourth most significant parameter, showing the importance of imperfections in the frame's geometry, even with the low COV of 1%. In addition, parameters H_{column}, H_{beam} and c_{cover} were the main and leading geometric parameters that control the frame response to the targeted design point. These results indicate the high influence of geometrical imperfections on the reliability of the RC structure. It was also noted that the depth of the concrete cover ranked high in importance, which is not surprising since its COV was 25% due to uncertainty in the construction of such structures. This finding may justify further investigation of the dispersion in the amount of cover in RC structures. The importance ranking of geometrical imperfections relative to other structural parameters indicated a significant influence of uncertain geometrical parameters on reliability assessments, even when the dispersion in the probability distribution is small.

These analyses can be used to minimise the total volume or the total expected cost of the structure subject to structural reliability constraints, to maximise the structural security subject to a given structural cost or simply to achieve a target structural reliability. This approach is particularly suitable for the possible implementation of geometric and material nonlinearities, the implementation of static and dynamic analysis, the simple coverage of aleatory (data-based) variability and epistemic (knowledge-based) uncertainty in terms of material and geometric characteristics, and earthquake time history records in the case of dynamic analysis. It is also possible to optimise significant Design Point-based parameters and define multiple LSFs during the same analysis, which can be based on local or global system responses, following internal forces and displacements or deformations. As a guideline for future researchers, for similar construction systems, it is enough to conduct FORM analysis, where importance vectors are available, while, for greater flexibility and especially parametric studies in earthquake engineering, we prefer the use of MCS. MVFOSM proved to be very proximate and as such incorrect for the nonlinear model response, while the two SORM variants did not contribute much to the accuracy of the reliability index.

Proceedings of the 2nd Croatian Conference on Earthquake Engineering - 2CroCEE
Zagreb, Croatia - March 22 to 24, 2023

DOI: https://doi.org/10.5592/CO/2CroCEE.2023.16

References

[1] Huang, C.; El Hami, A.; Radi, B. Overview of Structural Reliability Analysis Methods—Part I: Local Reliability Methods. Incert. Fiabil. Syst. Multiphys. 2017, 17, 1–10.
[2] Scott, M.H.; Fenves, G.L.; McKenna, F.; Filippou, F.C. Software Patterns for Nonlinear Beam-Column Models. J. Struct. Eng. 2008, 134, 562–571.
[3] Yaw, L.L. Co-Rotational Meshfree Formulation for Large Deformation Inelastic Analysis of Two-Dimensional Structural Systems. Ph.D. Thesis, University of California Davis, Davis, CA, USA, 2008.
[4] Denavit, M.D.; Hajjar, J.F. Description of Geometric Nonlinearity for Beam-Column Analysis in OpenSees; Technical report; Northeastern University: Boston, MA, USA, 2013.
[5] Rinchen; Hancock, G.J.; Rasmussen, K.J. Formulation and Implementation of General Thin-Walled Open-Section Beam-Column Elements in OpenSees; Technical Report 961; School of Civil Engineering, The University of Sydney: Sydney, Australia, 2016.
[6] Deng, J.; Gu, D.; Li, X.; Yue, Z.Q. Structural reliability analysis for implicit performance functions using artificial neural network. Struct. Saf. 2005, 27, 25–48.
[7] Haukaas, T.; Scott, M.H. Shape sensitivities in the reliability analysis of nonlinear frame structures. Comput. Struct. 2006, 84, 964–977.
[8] Hess, P.E.; Bruchman, D.; Assakkaf, I.A.; Ayyub, B.M. Uncertainties in Material and Geometric Strength and Load Variables. Nav. Eng. J. 2002, 114, 139–166.
[9] Buonopane, S.G. Strength and Reliability of Steel Frames with Random Properties. J. Struct. Eng. 2008, 134, 337–344.
[10] JCSS. Probabilistic Model Code Part III; Technical report; Technical University of Denmark, Joint Committee on Structural Safety (JCSS): Kongens Lyngby, Denmark, 2000.
[11] Celarec, D.; Ricci, P.; Dolšek, M. The sensitivity of seismic response parameters to the uncertain modelling variables of masonry-infilled reinforced concrete frames. Eng. Struct. 2012, 35, 165–177.
[12] Scott, M.H.; Haukaas, T. Software Framework for Parameter Updating and Finite-Element Response Sensitivity Analysis. J. Comput. Civ. Eng. 2008, 22, 281–291.
[13] Ellingwood, B.; Galambos, T.; MacGregor, J.; Cornell, C.A. Development of a Probability—Based Load Criterion for American National Standard A58; Technical Report; National Bureau of Standards: Washington, DC,USA, 1980.
[14] El-Reedy, M.A. Reinforced Concrete Structural Reliability; CRC Press, Taylor & Francis Group: Boca Raston, FL, USA, 2013; p. 369.
[15] Robertson, L.E.; Naka, T. Tall Building Criteria and Loading; American Society of Civil Engineers: New York, NY, USA, 1980; p. 900.
[16] Mishra, D.K. Compressive Strength Variation of Concrete in a Large Inclined RC Beam by Non-Destructive Testing; Technical report; Associated Cement Companies Ltd.: Mumbai, India, 1990.
[17] Obla, K. Variation in Concrete Strength Due to Cement—Part III of Concrete Quality Series. Improv. Concr. Qual. 2014, 9, 7–16.
[18] Sundararajan, C. Probabilistic Structural Mechanics Handbook: Theory and Industrial Applications; Springer: New York, NY, USA, 1995; p. 745.
[19] Bartlett, F.M.; MacGregor, J.G. Assessment of Concrete Strength in Existing Structures; Technical Report; Department of Civil Engineering, University of Alberta: Edmonton, AB, Canada, 1994.
[20] Haukaas, T.; Kiureghian, A.D. Finite Element Reliability and Sensitivity Methods for Performance—Based Earthquake Engineering; Technical report, Pacific Earthquake PEER Report 2003/14; Engineering Research Centre, PEER, University of California: Berkeley, CA, USA, 2004.
[21] EN 1990-1:2002. Eurocode 0—Basis of Structural Design; European Committee for Standardization, CEN: Brussels, Belgium, 2002.
[22] Porter, K.A.; Beck, J.L.; Shaikhutdinov, R.V. Sensitivity of Building Loss Estimates to Major Uncertain Variables. Earthq. Spectra 2002, 18, 719–743.
[23] Celarec, D.; Dolšek, M. The impact of modelling uncertainties on the seismic performance assessment of reinforced concrete frame buildings. Eng. Struct. 2013, 52, 340–354.
[24] Porter, K. A Beginner's Guide to Fragility, Vulnerability, and Risk; Technical report; University of Colorado Boulder; SPA Risk LLC: Denver, CO, USA, 2019.
[25] Lee, T.H.; Mosalam, K.M. Probabilistic Seismic Evaluation of Reinforced Concrete Structural Components and Systems; Technical report, PEER Report 2006/04; Pacific Earthquake Engineering Research Centre, College of Engineering, PEER, University of California: Berkeley, CA, USA, 2006.
[26] Huang, Y.; Whittaker, A.S.; Luco, N. Performance Assessment of Conventional and Base-Isolated Nuclear Power Plants for Earthquake and Blast Loadings; Technical Report MCEER-08-0019; University of Buffalo: Buffalo, NY, USA, 2008.